Parametric Pumping: Modeling Direct Thermal Separations of Sodium Chloride-Water in Open and Closed Systems

NORMAN H. SWEED and R. ALAN GREGORY

Princeton University, Princeton, New Jersey

Direct thermal parametric pumping separations of a NaCl-H_2O-ion retardation resin system have been investigated. Experimental breakthrough curves and batch parapump runs were used to determine the lumped-parameter mass transfer coefficient λ and its dependence on velocity and temperature. Computer simulation of additional batch runs verified both the model and the STOP-GO algorithm used to solve it. Computer estimates of open-system behavior are presented.

Parametric pumping is a general principle for separating fluid mixtures that takes particular advantage of unsteady state operation. Separation arises from the synchronous coupling of two alternating mass fluxes operating at right angles to each other. To be more specific, consider a two-phase system in which some species is distributed between the phases. Allow one phase to move past the other with an alternating velocity (that is, relative direction changes periodically). If we now cause the direction of an interphase flux of this species to alternate synchronously with the velocity, then we obtain a parametric pumping separation of the species, parallel to the alternating velocity (*1*).

Direct thermal parametric pumping, a process utilizing this principle, contains two phases—a solid adsorbent and a fluid mixture—arranged in a packed column through which the fluid moves back and forth. Alternating interphase transfer occurs by periodically changing the column temperature, thus altering the adsorption equilibrium. The result of these operations is the development of an axial concentration gradient.

Previously, Wilhelm and Sweed (*2*) performed a batch, direct thermal parapump separation of toluene and heptane and obtained a separation factor (that is, ratio of toluene concentrations in products) in excess of 10^5:1. The batch apparatus in Figure 1 shows that the fluid which leaves the column on one half cycle reenters the same end on the next half cycle with no product removed.

The separation capability of this total reflux arrangement suggests that partial reflux might also produce substantial separations but now with the added advantage of continual product removal.

We present here a model of a closed, batch, direct thermal parametric pumping system. Model parameters are estimated by mathematical simulation of experimental breakthrough curves and batch parapump separations. The model is then used to illustrate the behavior of a particular open continuous parapump system.

For the present study, we chose to separate aqueous solutions of NaCl using an ion retardation resin (Bio-Rad AG11A8) as the solid phase. Separations of NaCl-H_2O solutions by parapumping have been reported previously (*1, 3, 4*). However, these were all for the recuperative thermal mode in which a transient axial temperature profile is developed by maintaining the column reservoirs at different temperatures.

An ionic system, while inherently more difficult to model than a nonionic one because of electrical interactions, does offer several considerable advantages. Certainly the everincreasing demand for fresh water prompts us to consider this problem. Also, the availability of accurate, simple quantitative analytical methods for Na^+ and Cl^- is important. Finally, simple and inexpensive on-line monitoring of salt concentrations by electrical conductivity allows a more detailed study than does the system-disturbing removal of samples done previously (*2*).

Also, these previous parametric pumping investigations with NaCl all employed a mixture of ion exchange resins—one cationic, the other anionic—as the solid phase. Many problems were encountered using these resins, including the very low rates of mass transfer within the solid phase, the need for two different particles with different physical properties, and the difficulty of modeling the ion exchange process. We decided to eliminate these problems by using an ion retardation resin in which both cationic and anionic sites are mixed in the same particle and in which intraparticle mass transfer rates are considerably greater than previously obtained.

It should be noted that an open system has several additional degrees of freedom in its operation beyond those of the closed one. The feed location, feed rate, and the product drawoff rates are obvious choices, but additionally we must specify when in the cycle the column is to be fed and when product is to be removed. There is no requirement, for example, that feed be supplied continuously.

Because so many possible system variables and operating schemes exist, it would be difficult to study the open

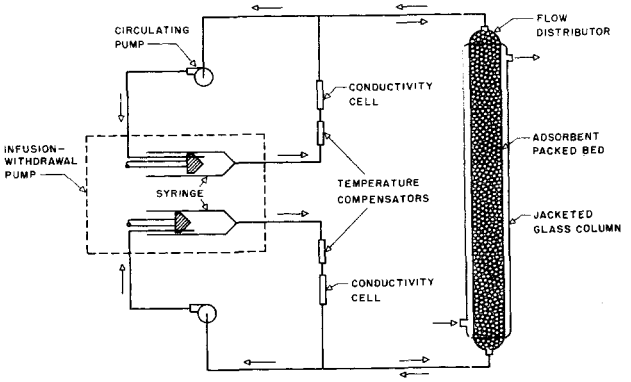

Fig. 1. Experimental arrangement for the closed direct thermal system.

R. Alan Gregory is with Union Carbide Corp., Bound Brook, New Jersey.

parapump system by experiment alone. Therefore we have modeled this system mathematically and can perform experiments on the computer.

THEORY

In direct thermal parametric pumping, the temperature of adsorbent particles changes throughout the entire bed synchronously with the change in flow direction. If we neglect axial and radial dispersion in the bed, we can write the following dimensionless fluid phase material balance:

$$\alpha f(t)\frac{\partial \phi_f}{\partial z} + \frac{\partial \phi_f}{\partial t} + \frac{\partial \phi_s}{\partial t} = 0 \qquad (1)$$

Although Equation (1) is valid for batch simulation, the velocity $\alpha f(t)$ may not be the same everywhere in the column for a nonbatch arrangement; indeed, in the open system, velocity will generally depend on whether the fluid is above or below the feed point. Hence for the open system we need a velocity which depends on both time and position, that is, $V(t, z)$.

To complete our model we need an expression for the rate of mass transfer between the phases:

$$\partial \phi_s/\partial t = R \qquad (2)$$

In general, R will be a function of fluid properties, adsorption equilibrium, solid properties, and fluid velocity.

Here we assume a rate expression which lumps the resistance to transfer at the particle surface even though the true resistance is a combination of intraparticle and interphase effects.* We further assume that the rate is proportional to the fluid concentration displacement from equilibrium. Experiments show the adequacy of this simple model. Thus

$$\frac{\partial \phi_s}{\partial t} = \lambda(\phi_f - \phi_f^*) \qquad (3)$$

The dimensionless mass transfer coefficient λ is the product of a dimensional coefficient h_m and the cycle time τ. Thus $\lambda = h_m\tau$.

Note that Equation (3) requires an adsorption isotherm relating solid and fluid concentrations at each operating temperature. In addition, we must supply initial and boundary conditions. These may be any which represent physically realizable values. Initial and boundary conditions for the batch parapump were presented previously (*1*).

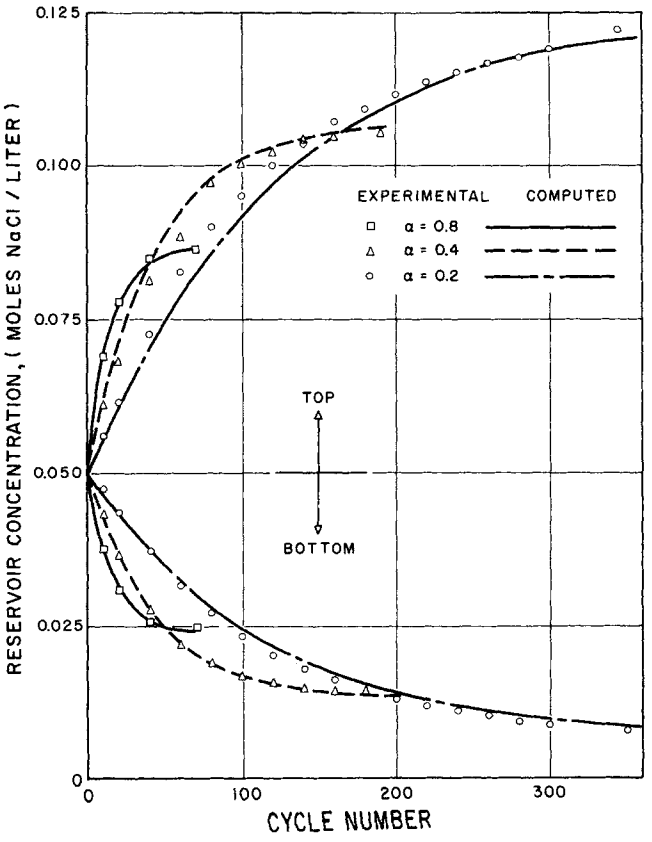

Fig. 2. Effect of α on reservoir concentrations of a closed system for an NaCl-H_2O solution with an ion retardation resin adsorbent. The cycle time is 20 min. The column is initially at equilibrium with 0.05M NaCl at 25°C. and operates at 5° and 55°C.

CLOSED SYSTEM

Apparatus

Experimental data obtained from a closed parapump system were used in conjunction with computational simulation to determine parameters in the model equations. We require an experimental system consistent with the assumptions used to derive the model eqautions. For example, the model assumes no radial heat transfer lag when temperatures switch each half cycle. We therefore constructed our column of such diameter that this lag time is small with respect to the minimum cycle time used, $\tau = 20$ min. In our column the mean temperature (measured experimentally) reaches 90% of its final value within 2 min. after a half cycle begins. The effect of this heating lag is reduced by a 30-sec. lag until flow begins (for the 20-min. cycle). Thus the column temperature is 90% of its final value in 15% (1.5 min.) of the shortest half cycle, $\tau/2 = 10$ min. This is the worst case.

The apparatus, shown in Figure 1, consists of a jacketed glass column ($L = 60$ cm., I.D. $= 1.1$ cm.) with reservoirs at each end. These reservoirs are 50-cc. plastic syringes driven by a Harvard infusion-withdrawal pump. Electrical conductivity flow cells were placed in each reservoir to monitor their concentrations continuously. In preliminary runs these cells indicated poor mixing in the reservoirs. The boundary conditions we used, however, assume well-mixed reservoirs (*1*). Therefore mixing loops were installed in each reservoir (using Gorman-Rupp oscillating pumps) to circulate the fluid out the front of the syringe, through the conductivity cell and its temperature compensator, and into the back of the syringe. The volume of each reservoir (the syringe plus circulating loop) is about 50 ml. when the syringe is full. The circulation rate is about 25 ml./min. The conductivity of each reservoir is recorded for the half cycle when the fluid flows from that reservoir into the column. A cyclic timer switches between conductivity cells. These measurements showed that the fluid entering the column was uniform during each half cycle.

To check the accuracy of the conductivity measurements, we analyzed the contents of the reservoirs at the end of each run using the Fajan method for Cl^- and flame spectrophotometry for Na^+.

EXPERIMENTAL DATA

The closed-system apparatus is used to obtain data in the range of operating conditions used in the open system. Therefore the closed system provides an experimental framework to test our model equations.

The temperature range of a parapump system is restricted by the boiling and freezing points of the solution or the heat transfer medium. It may be limited even further if degradation of either adsorbent or solute occurs at high temperatures. We chose the range of 5° to 55°C.

* A stirred-batch experiment indicated that the intraparticle diffusion coefficient was approximately 5×10^{-6} sq. cm./sec. A criterion, similar to one developed by Helfferich (*8*), was used to differentiate between particle and film diffusion control. Our system is film controlled at high concentrations and a combination of film and particle controlled in the lowest concentration ranges used.

to allow reasonable separation and yet minimize resin degradation in the course of extended experimentation. The column was hot during upflow and cold on downflow.

Effect of Displacement, α

The model equations for the closed system include the dimensionless displacement, $\alpha = \bar{v}\tau/L$, where $\bar{v}$ is the average fluid velocity per half cycle and L is the length of the bed.* Physically, α represents the total volume of fluid displaced per half cycle, divided by the volume of fluid in the column. It has been predicted computationally that separations at limiting conditions (that is, after many cycles) increase with a decreasing α (5); Figure 2 shows the first experimental verification of this effect. The α effect is explored in detail following a discussion of closed-system simulation.

We will show too that these data provide an additional verification of the model equations for the closed system.

Effect of Cycle Time, τ

The rate of interphase mass transfer is a function of temperature, fluid velocity, and cycle time. However, since velocity is inversely proportional to cycle time for fixed displacement, a study of cycle time alone includes implicitly the velocity effect. Figure 3 shows the top and bottom reservoir concentrations for three cycle times with $\alpha = 0.80$. Longer cycle times cause increased separations because more time is allowed for transfer to occur between phases.

* In this paper, α is twice the value of the variable α used in reference 6.

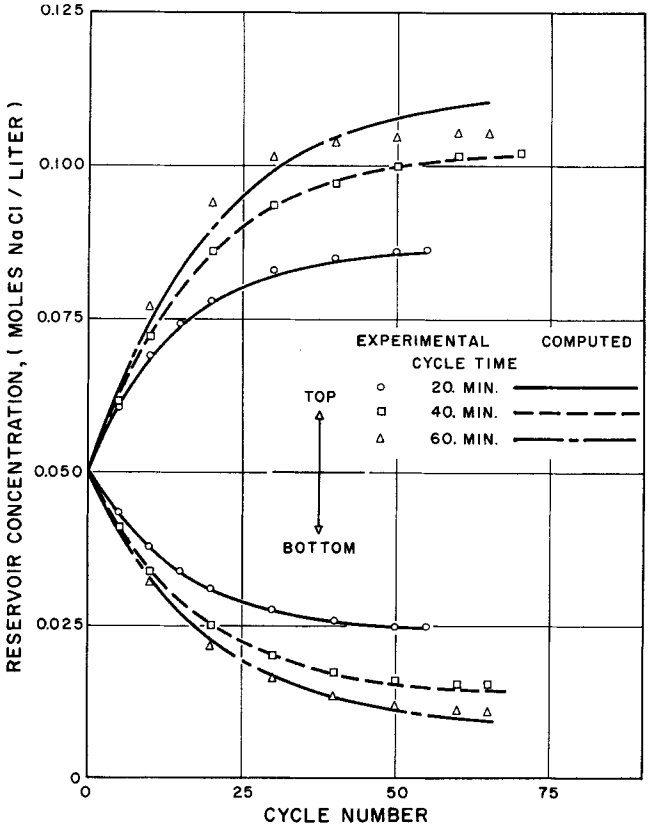

Fig. 3. Effect of cycle time τ on reservoir concentrations of a closed system for an NaCl-H_2O solution with an ion retardation resin adsorbent. The column is initially at equilibrium with 0.05M NaCl at 25°C and $\alpha = 0.8$. The system operates at 5° and 55°C.

Table 1. Equilibrium Isotherms at Two Temperatures for Aqueous NaCl Solutions of Bio-Rad AG11A8 Resin

$c_s = dc^*$ $\quad c^* \leq 0.06\ M$ NaCl
$c_s = ac^* + b$ $\quad c^* \geq 0.06\ M$ NaCl

	5°C.	55°C.
a	1.711	1.169
b	0.0225	0.0212
d	2.086	1.523

EQUILIBRIUM AND RATE DATA

Equilibrium isotherms for use in the rate expression, Equation (3), were determined by contacting a known amount of NaCl in solution with a known amount of initially solute-free resin at constant temperature. After equilibrium was reached, the fluid concentration was determined and the solute within the resin calculated by a mass balance. For the purposes of our model equations, the concentration of the solid phase includes all solute within the resin particle—both adsorbed and in the pore fluid. Figure 4 shows the isotherms obtained for 5° and 55°C.

The model equations make no assumptions about the form of the equilibrium function. These equations require only continuous equilibrium values; thus any convenient interpolation curve can be used. Figure 4 shows also each isotherm approximated by two straight lines intersecting at an arbitrary point. These linear functions were used in all calculations (Table 1). A more complex curve showed almost no difference and caused only increased computation time.

A rate experiment is necessary to determine the validity of the assumed interphase transfer expression, and its dependence on temperature and velocity. Several techniques for studying rates are available, including isothermal

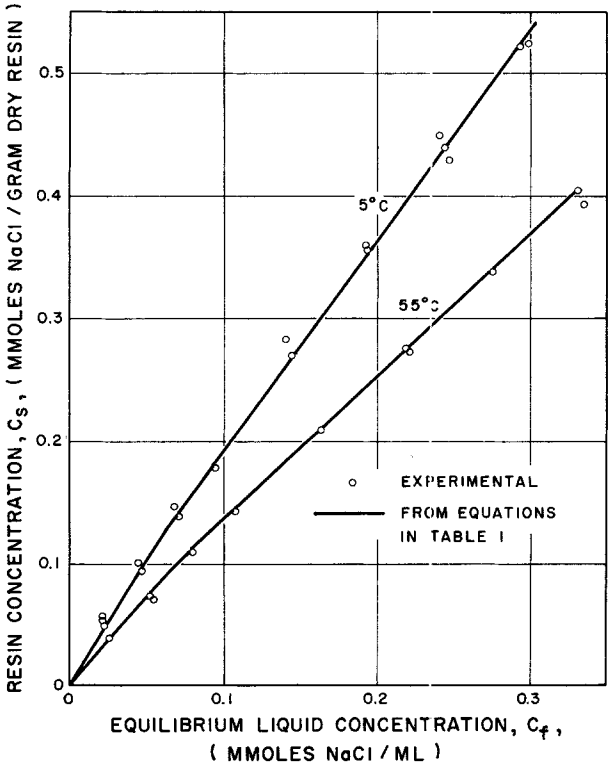

Fig. 4. Equilibrium distribution of NaCl between the aqueous solution and the solid adsorbent AG11A8 ion retardation resin. The computed lines are from the equations in Table 1.

breakthrough, differential bed, and stirred-batch reactor experiments. Batch reactor experiments are not suitable for modeling column data because we cannot correlate the external fluid velocity in a stirred tank with that in a packed bed.

While the differential bed can give us good rate information, we chose instead the breakthrough curve method because it is more like parametric pumping. The model equations for a half cycle of parapumping are identical to those for calculating a breakthrough curve except for initial conditions. Thus if we can simulate the breakthrough curves we can be confident that the parapump model is valid and that our solution of it is correct.

The simple linear fluid-phase driving force in Equation (3) implies a film-controlled mechanism, although it can also be viewed as simply an empirical expression. Experimental breakthrough data for both saturation and elution were collected at the highest flow rate to be used in either the closed or open systems. If the film mechanism is valid at this highest flow rate, then lower flow rates should also follow the same mechanism. Figure 5 shows the saturation breakthrough curves for both 5° and 55°C.

The model Equations (1) and (3) were solved using the STOP-GO algorithm (6). The computed curves in Figure 5 were obtained by fitting λ to the experimental data. The fit is quite adequate for our purposes, so we accept this simple rate expression for our model.

It is significant that the relatively efficient STOP-GO algorithm adequately solved the breakthrough problem. The size of the position and time increments for all cases was $\Delta z = \Delta t = 0.02$. Using increments of one-half this value had a negligible effect on the simulation of the breakthrough curves. Such solutions are often difficult because the axial concentration gradients encountered in this situation are severe. Modeling the breakthrough data lends confidence to the validity of the model when applied to parametric pumping.

The breakthrough curves provide values of λ for the highest flow rate. If we assume the temperature and velocity dependence of λ is similar to that for the j factor correlations for packed beds (7), then changing flow rate does not affect the temperature dependence of λ. Hence the ratio, $\lambda(T_{HOT})/\lambda(T_{COLD})$, is a constant for all flow rates. λ does vary with flow rate, however.

SIMULATION OF THE CLOSED SYSTEM

The following approach was used to simulate the closed system. From breakthrough experiments we obtained the temperature dependence of λ in the form of a ratio $\lambda(T_{HOT})/\lambda(T_{COLD})$. The velocity dependence is determined using closed-system runs of varying cycle time but constant α. Two runs with different α's then provide an independent check of the complete model. Alternatively, more breakthrough experiments could have been made to determine the velocity dependence of λ. Howver, by using the closed-system runs for this purpose, we lump any additional effects into λ which have not been previously included. For example, the periodic concentration boundary condition around particles of resin in the bed can cause a buildup of concentration waves in the particles. This has been shown to have a significant effect on separation when intraparticle diffusion controls (3). By using a parapump system instead of breakthrough curves we can lump these effects into λ.

The rate parameters obtained from breakthrough data had the same velocity and temperatures as the $\alpha = 0.80$, $\tau = 20$ min. batch parapump run of Figure 3. These closed-system data were more sensitive to small changes

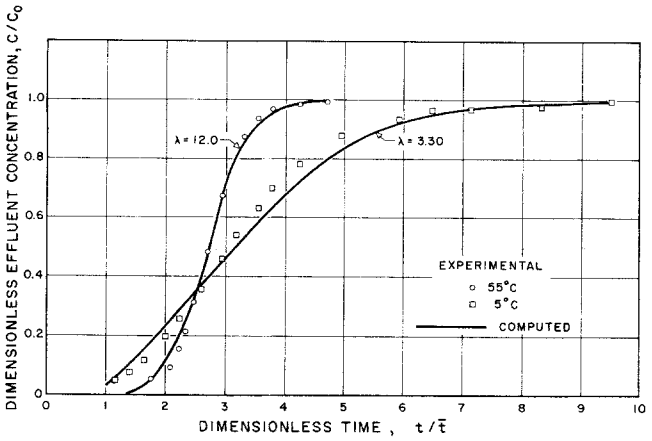

Fig. 5. Saturation breakthrough curves for the NaCl-H_2O-ion retardation resin with a feed concentration C_0 of 0.10M NaCl and a velocity equivalent to that in a closed system with $\tau = 20$ min. and $\alpha = 0.8$. The residence time $\bar{t}$ is the void volume divided by the volumetric flow rate.

in the λ's than were the breakthrough curves. Hence the breakthrough data were used to estimate the ratio of the λ's, with final adjustments made to fit the $\tau = 20$ min. data as closely as possible.

Next, the parametric pumping separation runs with cycle times of 20, 40, and 60 min. were used to determine the velocity dependence of λ. From the dimensionless equations for a closed system we have said that $\alpha = \bar{v}\tau/L$ and $\lambda = h_m\tau$. If we assume a correlation for h_m in the form of the j factor (7), then

$$h_m = j \cdot v \tag{4a}$$

where

$$j = K_1(T) \cdot N_{Re}{}^{-a} \tag{4b}$$

or

$$j = K_2(T) \cdot v^{-a} \tag{4c}$$

where K_1 and K_2 are functions of temperature.

Combining Equations (4a) and (4c)

$$h_m = K_2(T)v^{1-a}$$

Then

$$\lambda = K_2(T)v^{1-a}\tau \tag{4d}$$

For a given α and column length L, a square-wave velocity (that is, $v = \bar{v}$) is inversely proportional to τ. Hence, using the definition of α

$$\lambda = K_2(T)v^{1-a}\left(\frac{\alpha L}{v}\right)$$

or

$$\lambda = K_3(T)\alpha v^{-a} \tag{5}$$

The breakthrough curves at one velocity and two temperatures provide two λ's, the ratio of which [from Equation (5)] is

$$\frac{\lambda(T_{HOT}, v)}{\lambda(T_{COLD}, v)} = \frac{K_3(T_{HOT})}{K_3(T_{COLD})} \tag{6}$$

Then, by making batch parapump runs at constant α, the same hot and cold temperatures [thus from Equation (6) the same ratio of the λ's], and different cycle times (hence different velocities), λ's can be found by matching simulated and experimental separations.

From the definition of α

$$\frac{v_2}{v_1} = \frac{\alpha_2\tau_1}{\alpha_1\tau_2} \tag{7}$$

Table 2. Values for the Rate Parameter λ Determined from Breakthrough and Batch Data in the Case of $\tau = 20$ Min. and from Simulation of Batch Separations for $\tau = 40, 60$

τ, min.	α	λ(55°C.)	λ(5°C.)
20	0.8	12.0	3.30
40	0.8	19.5	5.35
60	0.8	25.8	7.11

Combining Equations (5) and (7)

$$\frac{\lambda}{\lambda_B} = \left[\frac{K_3(T)}{K_3(T_B)}\right]\left[\frac{\alpha}{\alpha_B}\right]^{1-a}\left[\frac{\tau}{\tau_B}\right]^{a} \qquad (8)$$

where the subscript B refers to the breakthrough curve data.

The first factor on the right-hand side of Equation (8) is determined from Equation (6).

We have used the λ's (Table 2) which simulate the experiments of Figure 3 to determine a value of $a = 0.7$. The velocity dependence of the dimensionless rate parameter λ is thus characterized by this exponent.

As an independent check of the computer model, the fluid-phase driving force, and the temperature and velocity dependence of λ, we attempted to simulate two additional experimental runs a priori. In these runs we varied the parameter α. Equation (8) predicts that at constant τ, λ decreases with decreasing α. It has been shown previously (6) that when λ does decrease, so does separation. Hence we might expect a drop in separation as α becomes smaller. The experimental evidence presented above (Figure 2), however, shows the opposite behavior. Thus, there must be an α effect which overshadows the change in λ. Clearly, if α is greater than one, fluid moves from one reservoir, through the column, and into the other reservoir with mixing and less separation as a result. When α is less than one, mixing no longer occurs directly between the reservoirs. Rather an indirect mixing occurs which depends on the existence of nonsharp axial concentration profiles such as occur with finite λ. Because of these profiles the concentration of the column effluent changes continuously during a half cycle. Over most ranges of λ, including those used here, the top effluent concentration decreases as the less concentrated regions of the axial profile exit the column. At the bottom of the column the reverse is true with effluent concentration increasing. Thus at larger α, more of the profile leaves the column, decreasing separation and overshadowing the effect of the increased λ.

There are values of the interphase mass transfer coefficient (λ small) where the effluent concentration at the top first increases and then decreases as more fluid exits the column. In this case the dependence of separation on α is not monotonic.

It is significant that the α effect is accurately predicted from the model equations (Figure 2). Also, the α effect disappears at the limits $\lambda = 0$ and $\lambda = \infty$ since in these cases concentration fronts are nonexistent or sharp, respectively. Using Equation (8) we predicted the values for λ shown in Table 3. Figure 2 shows both experimental and simulated separations for these runs. Agreement is excellent.

Table 3. Values of the Rate Parameter λ Calculated Using Equation (5) and Used in Figure 2

τ, min.	α	λ(55°C.)	λ(5°C.)
20	0.8	12.0*	3.30*
20	0.4	9.75	2.68
20	0.2	7.91	2.18

* These values are from Table 2.

OPEN-SYSTEM SIMULATION

An open parapump system receives as feed a solution which it separates into two (or more) product streams. After the initial transients have disappeared, the mixed average concentrations of these products become steady for succeeding cycles. Cycle time is still defined in the open system since it retains the periodic characteristics of parametric pumping.

Introduction of feed and withdrawal of products allow the staging of several open parapump columns. Of course, each individual column has several more degrees of freedom than the batch. For example, the feed for a given column can be located at either end or at some intermediate position. The concept of reflux can be introduced by allowing some fluid to be withdrawn as product while some is saved in a reservoir to flow back into the column later. Reflux between columns in a staged system is also possible.

How we operate the open system depends on our separation objective. For example, if we want to concentrate solute we would construct one kind of parametric pumping system, while purification of solvent would require a different system.

The variety of possible open parapump systems is so large as to discourage a broad experimental program. Therefore we have used the model developed for the closed system to investigate computationally the behavior of open systems.

We have modeled one specific open system by using the equations and parameters of the closed system. There has been no attempt at optimization. A schematic for one full cycle of this system, Figure 6, shows a packed column with reservoirs at each end. In this case the column is cooled while flow is from top to bottom, and heated during upward flow. Product is withdrawn at both the top and bottom of the column; all feed is introduced at the top. Each column shows the flow in one portion of the

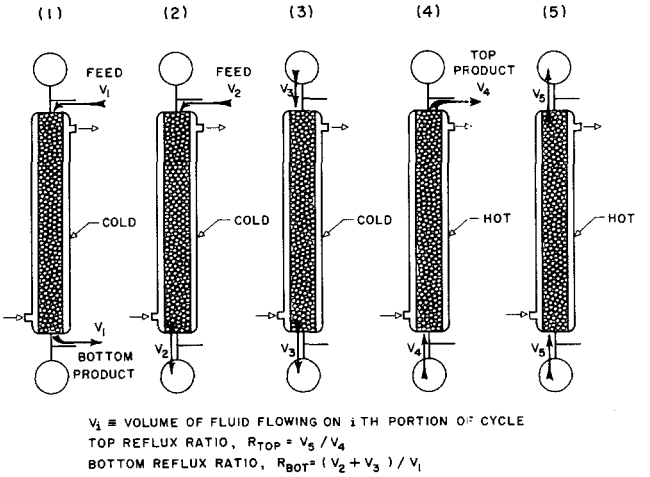

Fig. 6. Schematic of a particular open direct thermal system. Flow sequences for one cycle: (1) feed V_1 and collect V_1 as bottom product, (2) feed V_2 and collect V_2 in bottom reservoir, (3) flow V_3 from top reservoir and collect V_3 in bottom reservoir, (4) flow V_4 from bottom reservoir and collect V_4 top product, and (5) flow V_5 from bottom reservoir and collect V_5 in top reservoir. Column cold during (1) to (3) and hot during (4) and (5).

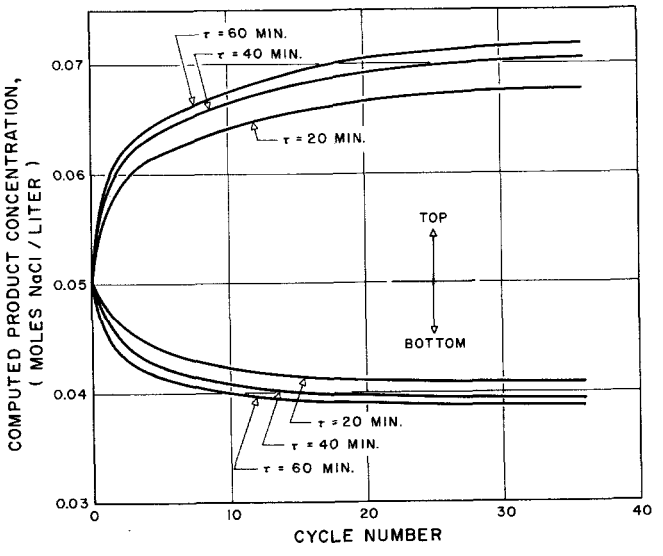

Fig. 7. Computed effect of cycle time on the product concentrations for the open system illustrated in Figure 6. For these runs $\frac{1}{2}\sum_{i=1}^{5} V_i$ is 80% of the void volume, $R_{TOP} = 1.0$, $R_{BOT} = 1.0$. Other operating conditions are the same as in Figure 3.

cycle, each portion occurring sequentially as numbered. The volumetric flow rate in the bed is the same magnitude throughout the cycle and is determined from the total volume flowed

$$V_{TOT} = \sum_{i=1}^{5} V_i$$

divided by the cycle time τ, where V_i is the volume of fluid flowed on the i^{th} portion of the cycle. Reflux ratios are defined at each end of the column as the volume of fluid collected in the reservoir per cycle divided by the volume of product per cycle at that end.

Velocity dependence of the mass transfer parameter λ is assumed the same as in the closed system.

Simulations of this system for several different cycle times are shown in Figure 7. These results include the transients from an equilibrium initial condition at 25°C. with a 0.05 M NaCl fluid concentration. Thus, for $\tau = 20$ min. and feed at 0.05 M NaCl, after the transients have died away, top product is withdrawn at 0.068 M NaCl and bottom product at 0.041 M NaCl. For simulations in Figure 7 R_{TOP} and R_{BOT} are each set at 1.0; half the total volume flowed, $V_{TOT}/2$, is 80% of the column void volume (which results in a fluid velocity equal to that of a closed system with $\alpha = 0.80$ and $\tau = 20$ min.). There is no net change in the reservoir volumes from cycle to cycle. Thus the volume of product per cycle is the same for each of the several cycle times used. Separation increases with cycle time, but the volume of product decreases on a real time basis.

CONCLUSION

We have developed a model which simulates the experimental behavior of a closed parametric pumping system. Separately determined interphase rate parameters for each temperature in the cycle were necessary for proper description of the system. We have used the model to illustrate the behavior of a particular open parapump system. The feasibility of using an open system for separation is shown in this example. With the model equations now available, optimization schemes can be used in a broad investigation of open parapump systems.

ACKNOWLEDGMENTS

We thank T. J. Butts for valuable discussions and J. E. Sabadell for her assistance with analytical work. We are indebted to the late Richard H. Wilhelm for innumerable contributions to this study.

Financial support was provided by the National Science Foundation under Grant GK-1427X1. Computations were performed at the Princeton University Computer Center, which is supported in part by National Science Foundation Grants GJ-34 and GU-3157.

We also thank R. W. Rolke for his comments on an earlier draft of this paper.

NOTATION

C_0 = fluid phase feed concentration, moles/liter
C^* = fluid concentration in equilibrium with the solid phase, moles/liter
C_s = solid phase concentration, mmoles/g. dry resin
$f(t)$ = fluid velocity in closed system, dimensionless
h_m = interphase mass transfer coefficient, min.$^{-1}$
K_1, K_2, K_3 defined by Equations (4) and (5)
L = length of packed bed, cm.
N_{Re} = Reynolds number, dimensionless
R = interphase mass transfer rate, dimensionless
T = temperature, °C.
t = time, dimensionless
$\bar{t}$ = residence time of packed bed, dimensionless
v = fluid velocity, cm./sec.
$\bar{v}$ = fluid velocity averaged over one cycle, cm./sec.
V_i = volume of fluid flowed on i^{th} portion of open system cycle
$V(t, z)$ = fluid velocity in open system, dimensionless
V_{TOT} = total volume of fluid flowed, $\sum_{i=1}^{5} V_i$
z = axial position in packed bed

Greek Letters

α = dimensionless displacement
λ = interphase mass transfer coefficient, $h_m\tau$, dimensionless
ϕ_f = fluid phase concentration, dimensionless
ϕ_f^* = fluid concentration in equilibrium with the solid phase, dimensionless
ϕ_s = solid phase concentration, dimensionless
τ = cycle time, min.

LITERATURE CITED

1. Wilhelm, R. H., A. W. Rice, R. W. Rolke, and N. H. Sweed, *Ind. Eng. Chem. Fundamentals*, 7, 337 (1968).
2. Wilhelm, R. H., and N. H. Sweed, *Science*, **159**, 522 (1968).
3. Rolke, R. W., and R. H. Wilhelm, *Ind. Eng. Chem. Fundamentals*, 8, 235 (1969).
4. Wilhelm, R. H., A. W. Rice, and A. R. Bendelius, *ibid.*, 5, 141 (1966).
5. Sweed, N. H., Ph.D. dissertation, Princeton Univ., N. J. (1968).
6. ———, and R. H. Wilhelm, *Ind. Eng. Chem. Fundamentals*, 8, 221 (1969).
7. Bird, R. B., W. E. Stewart, and E. N. Lightfoot, "Transport Phenomena," Wiley, New York (1960).
8. Helffrich, F., "Ion Exchange," McGraw-Hill, New York (1962).

Manuscript received September 5, 1969; revision received December 1, 1969; paper accepted December 4, 1969.